

A non-contact optical technique for vehicle tracking along bounded trajectories

This content has been downloaded from IOPscience. Please scroll down to see the full text.

2015 J. Phys.: Conf. Ser. 658 012010

(<http://iopscience.iop.org/1742-6596/658/1/012010>)

View [the table of contents for this issue](#), or go to the [journal homepage](#) for more

Download details:

IP Address: 217.112.157.21

This content was downloaded on 14/05/2017 at 18:18

Please note that [terms and conditions apply](#).

You may also be interested in:

[Non-contact optical Liquid Level Sensors](#)

L.L. Kiseleva, L.V. Tevelev and R.R. Shaimukhametov

[Development of non-contact laser vibrometer](#)

I Kononov, E Velichko and E Aksenov

[Non-contact surface resistivity measurement for materials greater than \$10^9 \Omega\$](#)

Toshiyuki Sugimoto and Koichi Taguchi

[New Approach for Non-Contact Measurement Using Vision Probe](#)

P B Costa, F O Baldner, J F S Gomes et al.

[Passively-Switched, Non-Contact Energy Harvester for Broad Operational Range and Enhanced Durability](#)

William Z Zhu and Carol Livermore

[A 2D mark shearing technique for characterizing the mechanical properties of material](#)

Tao Hua, Huimin Xie, Fulong Dai et al.

[Non-Contact, No Wafer Preparation Deep Level Transient Spectroscopy Based on Surface Photovoltage](#)

Jacek Lagowski, Andrzej Morawski and Piotr Edelman

[Non-contact Ultrasonic Velocity Measurement of Plastics by Sing-Around Method: Stress Effect and Anisotropy](#)

Tohru Imamura

[Injection Level Spectroscopy: A Novel Non-Contact Contamination Analysis Technique in Silicon](#)

George Ferenczi, Tibor Pavelka and Péter Tüttő

A non-contact optical technique for vehicle tracking along bounded trajectories

S Giancola¹, H Giberti¹, R Sala¹, M Tarabini¹, F Cheli¹, M Garozzo²

¹ Department of Mechanical Engineering, Politecnico di Milano, Milano, Italy

² SINECO S.p.a., Milano, Italy

E-mail: silvio.giancola@polimi.it

Abstract. This paper presents a method for measuring the non-controlled trajectory of a cart along a bounded rectilinear path. The method uses non-contact measurement devices to identify the position of a movable laser scanner working in helical mode in order to reconstruct the 3D model of bridges. The main idea of the proposed method is to use vision systems in order to identify the coordinates of the laser scanner placed on the cart with respect to the global reference system. A fit-to-purpose vision system has been implemented: the system uses three CCD's cameras mounted on the cart to identify the relative rotations with respect to the environment. Two lasers pointers and a laser distance meter are fixed at the starting point of the trajectory and pointing in the direction of motion of the cart, creating three dots on a plane placed on the cart. One of the camera detects the cart displacements and rotations in the plane using a blob analysis procedure. The method described in this paper has a constant uncertainty and the measurement range only depends on the lasers power. The theoretical accuracy of the measurement system is close to 1 mm for the translation along the motion direction and around 0.5 mm along the other two directions. Orientations measurement have a theoretical accuracy of less than 0.1 °. The solution has been implemented for the 3D reconstruction of concrete bridge; preliminary experimental results are presented and discussed.

1. Introduction

There are several literature studies focused on the inspection techniques for the 3D reconstruction of concrete bridges; recently, Giberti [1] and Zanone [2] proposed a novel technique for concrete bridge inspection with the aim of providing a complete reconstruction of the three dimension (3D) geometry of a concrete bridge using a 3D laser scanner. The latter is an instrument which reconstructs the 3D environment through a spherical scan, with two controlled motors guiding a laser distance meter in all the directions in order to acquire a dense point cloud in a few minutes. Blocking one of the motors, it is possible to obtain a helical scan, that is only a section of the surrounding environment. Registering multiple sections through a path tracking system, it is possible to dynamically acquire a cloud of points, moving the instrument around the structure. The measurement chain has been derived from the previous studies: the laser scanner is mounted on the moving cart: the by-bridge model is schematized in Figure 1 and the carrying system is shown in Figure 2 .



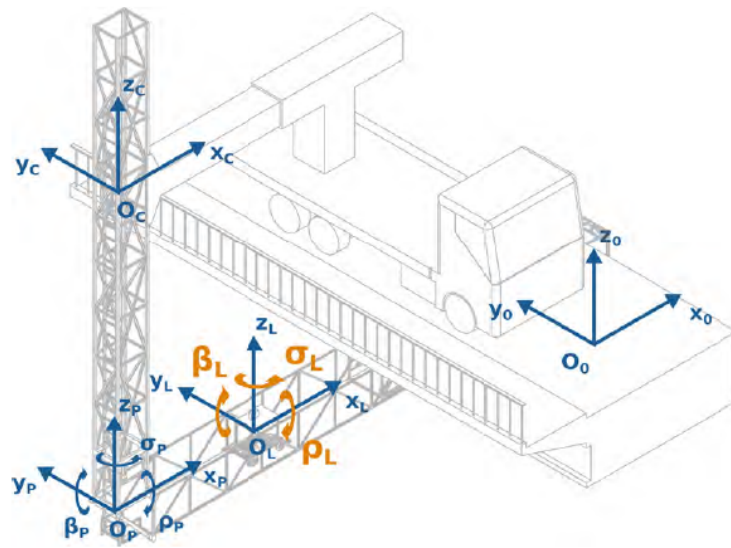


Figure 1. Model of the by-bridge where the carrying system is running

Zanone [2] presented a measurement chain based on a custom computer vision system for the identification of the laser scanner position. The measurement chain is composed by:

- (i) An incremental encoder on the truck that measures the truck movement on a forward direction,
- (ii) A vision system at the base of the vertical part of the inspection by-bridge, based on two laser beams and a camera that measures the motion of the projected dots at the bottom,
- (iii) A similar vision system on board of the cart, in order to measure the transverse movements and the roll angle,
- (iv) Another incremental encoder on the cart in order to measure its longitudinal displacement,
- (v) An uniaxial servo-inclinometer in order to measure the pitch angle of the carrier.



Figure 2. CAD of the carrying system for the laser scanner designed in [1]

Experimental results outlined that the accuracy of the measurement system was limited by the incremental encoder and by the servo-inclinometer, because of the presence of slipping on the traction wheels and of the shocks due to the fast movement of the cart along the by-bridge. Finally, the lack of information about the cart yaw orientation prevent from detecting the accurate orientation of the laser scanner in the fixed reference system.

This paper presents a novel technique for the identification of the cart trajectory and orientation, but it can be generalized on every vehicle that has a quasi-rectilinear motion. The aim of the proposed method is to reduce the criticalities evidenced in the previous works, in particular:

- to reduce the uncertainty of the position in the direction of the vehicle motion,
- to measure the orientation of the cart (yaw and pitch angles).

The proposed system is based exclusively on optical techniques: the accuracy of the distance is reduced by adopting a laser distance meter and the orientation is detected with vision-based systems.

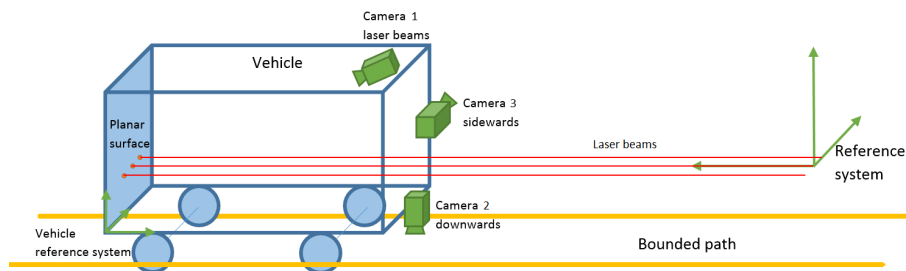


Figure 3. Scheme of our system for the vehicle tracking along the bounded path

As shown in Figure 3, three laser beams are placed at the beginning of the walkable section of the by-bridge. The central one is the laser distance meter, while the other two are used as optical rails. The three lasers are aligned in the direction of the motion of the cart. The distance meter measures the displacement along the bounded path and camera 1 (see Fig. 3) measures the positions of the lasers onto a planar side of the vehicle, which reconstructs the other two displacements and the roll angle of the vehicle. On the ground, a straight line is drawn along the bounded path and is captured by camera 2. The yaw angle is measured with an algorithm of edge detection. On the side, the handrail is used as reference for the measurement of the pitch angle through camera 3.

As any vision systems, the identification of the best parameters for the edge and blob detection is crucial.

In this paper, we first present the state of the art for different position tracking systems. Then, the proposed technique is explained in details and applied to the problem of 3D reconstruction of bridges. Finally, preliminary results are presented and discussed from a metrological point of view.

2. State of the art

There are different solutions for the identification of the identification of objects' trajectories. The most common is probably the Global Positioning System (GPS), that provides an absolute position tracking, thanks to a triangulation with stationary satellites, but other solutions such as the Inertial Measurement Unit (IMU) and the vision system are nowadays available.

2.1. Global Positioning System

The GPS identifies the objects' positions using the triangulation technique through multiple satellites in stationary orbit around the Earth. The main limitations to the use of GPS is that the quality of the signal below the bridge is definitely poor and the accuracy of standard systems (in the order of a few meters) is not sufficient to accurately identify the position of the cart on the by-bridge.

2.2. Inertial measurement unit

IMU are usually set-up by three accelerometers, three gyroscopes and sometimes three magnetometers and are commonly used in many applications, from smartphones to spacecrafts. IMU are usually coupled with a GPS to compensate their known drift problems; this issue, evidenced in the previous experimental campaign, prevented their use in the proposed device.

2.3. Vision techniques

There are different vision techniques that can be used in motion tracking problems. Generally, they can be divided in two categories:

- the use of vision systems as an external tool, for the measurement of the motion of an object in an environment,
- the use of vision systems as a visual tool for the object, for the measurement of its "egomotion".

Pattern matching techniques belong to the first category and are usually implemented for the tracking of objects, in both 2 or 3 dimensions. A possible alternative is represented by trinocular stereoscopic systems, which use known markers placed on the cart and a fixed camera to track their position. Preliminary tests performed in our laboratory ([3, 4, 5]) evidenced the worsening accuracy of 3D reconstruction at the increasing of depth (the farer the object is, the less accurate is the reconstruction).

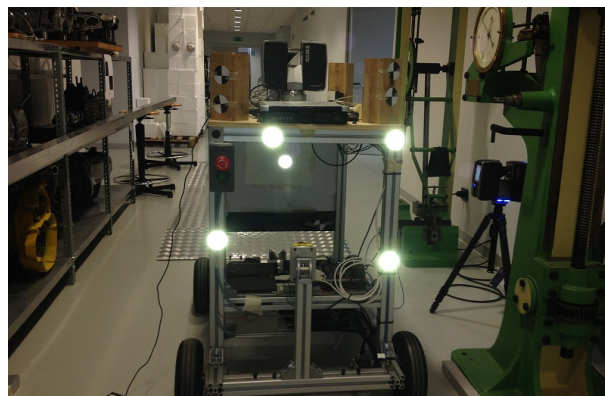


Figure 4. Carrying system with reflective markers for the tracking with trinocular vision system

Simultaneous Localization and Mapping (SLAM) belong to the second category (egomotion in an unknown environment). The typical application uses a 2D or 3D vision systems to recognize the surrounding world for the identification of its egomotion. There are different implementation of SLAM techniques; in this work we use this technique with 2D vision systems for the measurement of the yaw and pitch angles of the carrier.

3. Solution proposed

Our proposed optical solution for the identification of the cart trajectory is set-up with a laser distance meter, two laser pointers and an on-board camera (camera 1 on Fig. 3) observing the dots projected on a cart surface. This system measures the motion (the three translations x_L , y_L and z_L and the roll rotation ρ_L with respect to (O_p, X_p, Y_p, Z_p) reference system in Figure 1.

The second system is based on a single camera that measures the orientation of a line in the observation plane, in order to detect the rotation with the egomotion principle.

3.1. System {Lasers + Distance Meter + Camera 1}

This vision system consists of an optical bench supporting two laser pointers and a laser distance meter. The three laser beams are parallel and define the reference system for the measurement of the cart motion. The wavelength of the three lasers beams are 639 nm, corresponding to the red colour. As shown in Figure 5, the X-axis corresponds to the beam of the distance meter, the plane (O, X, Y) corresponds to the plane defined by the aligned laser beams and the Z-axis corresponds to the normal to this plane. The alignment between the three lasers is of paramount importance and has been experimentally verified as the deviation from parallelism at distances ranging from 2 to 30 m.

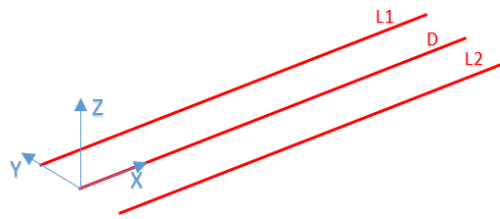
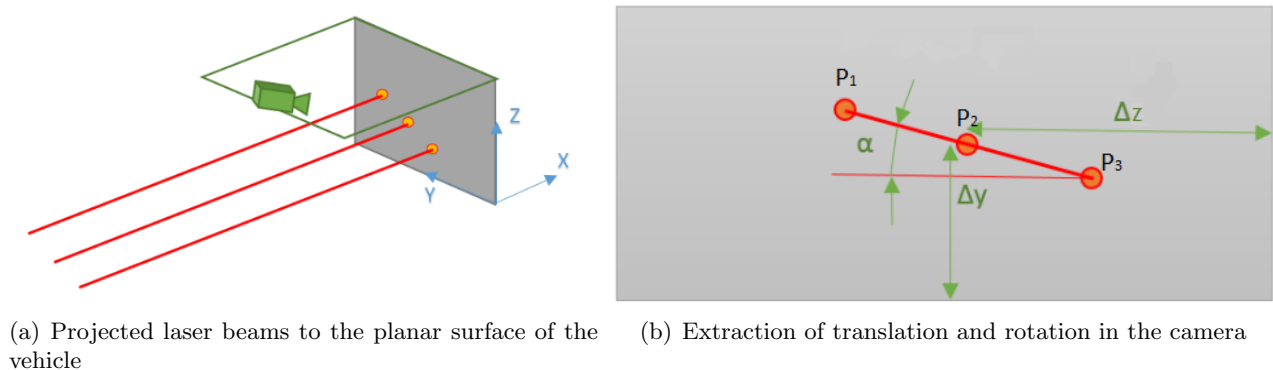


Figure 5. Definition of the reference system for the laser beams

The camera deputed to observe the 3 spots has a bandpass filter from 635 to 646 nm and is located on the cart in order to observe the three laser spots. The spots location has been identified with a blob detection algorithm. Since the camera sensor is not parallel to the observation plane, a preliminary calibration has been performed by observing a grid with known geometry, so that the result of measurement is an array of spots coordinates in physical units (mm).



(a) Projected laser beams to the planar surface of the vehicle (b) Extraction of translation and rotation in the camera

Figure 6. Elaboration for the system {Lasers + Distance Meter + Camera 1}

With this setup, the translation of the vehicle reference system is obtained by combining information from the camera and the distance meter. In particular, the distance meter detects

the distance along the X-axis and the camera captures translations along Y and Z axes. Rotations are measured by the different vision systems. The blob detection algorithm leverages on the classical image thresholding coupled with the blob analysis. As shown in Figure 6(b), the translation is detected by the position of the central dot (the distance meter), while the two spots of the laser pointers are used to detect the roll angle as described in the next section.

3.2. System {Camera + Line}

Yaw and pitch angles are measured by cameras located on the cart observing lines placed on the by-bridge, as shown in Figure 7(a).

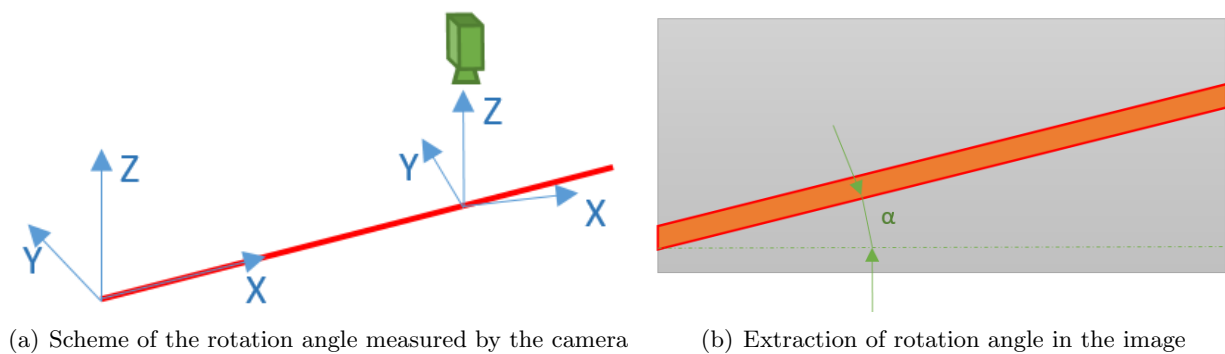


Figure 7. Elaboration for the system {Camera + Line}

A camera, mounted with an infrared lightning system and an infrared filter, measures the orientation angle of the line respect to the camera reference system. Also in this case, the camera underwent to a metrological calibration procedure in order to measure the angle in physical coordinates. Thanks to the edge detection algorithm, it is possible to identify the position of the line and the rotation angle between one system and the other.

This system has been used twice in our application, for the measurement of the pitch and the yaw angles.

4. Experimental Setup

In our measurement chain, this system is used for the estimation of the position of the carrier along the by-bridge walkway. This movement is characterized by six degrees of freedom, described by X_p , Y_p and Z_p in position and ρ_p , β_p and σ_p in rotation, as described in Figure 1. Due to the free but linearly bounded motion, the three angles can be considered as small.

4.1. {Lasers + Distance Meter + Camera 1}

The optical bench with the two laser pointers and the distance was mounted the beginning of the by-bridge walkway (Figure 8(a)). The lasers are mechanically aligned with a dedicated calibration procedure.

A camera uEye model "UI-5240CP-M-GC" manufactured by IDS (resolution of 1280x1024 pixels, frame rate 25 Hz) is rigidly fixed to the cart frame observing three spots' projection plane.



(a) Structure where the lasers and the distance meter are mounted (b) Projection of the lasers on the planar surface of the cart

Figure 8. Setup for the by bridge application

Images are stored by a LabVIEW-based software running on an embedded PC on the carrier and off-line processed. This solution allows a better system tuning for an optical identification of the blob detection parameters. The thresholding for the blob detection on the grayscale images was performed with a level of 30 on a 8-bit scale. The lookup region of interest (ROI) is set dynamically, since between an acquisition and the other the movement should not exceed 30 pixels ($\simeq 15$ mm in 40 ms). This allowed a reduction of the image processing time (order of a few milliseconds for each frame). Figure 9 shows the parameter of the blob detection, with the dark image in the centre, the dynamically set ROI in green, and the three points in red.

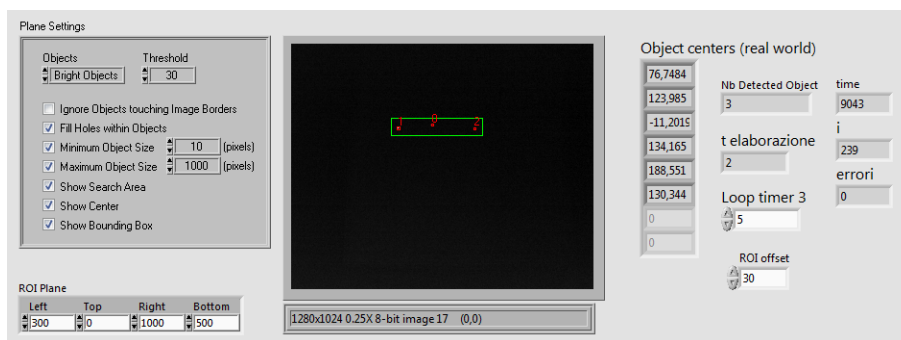


Figure 9. Labview interface for the blob detection

4.2. {Camera 2 + Line}

The {Camera + Line} system is used to detect both the pitch and the yaw of the cart. Yaw is detected by observing a metallic meter aligned with the walkway axis and with the three laser beams as shown in Figure 10(a).

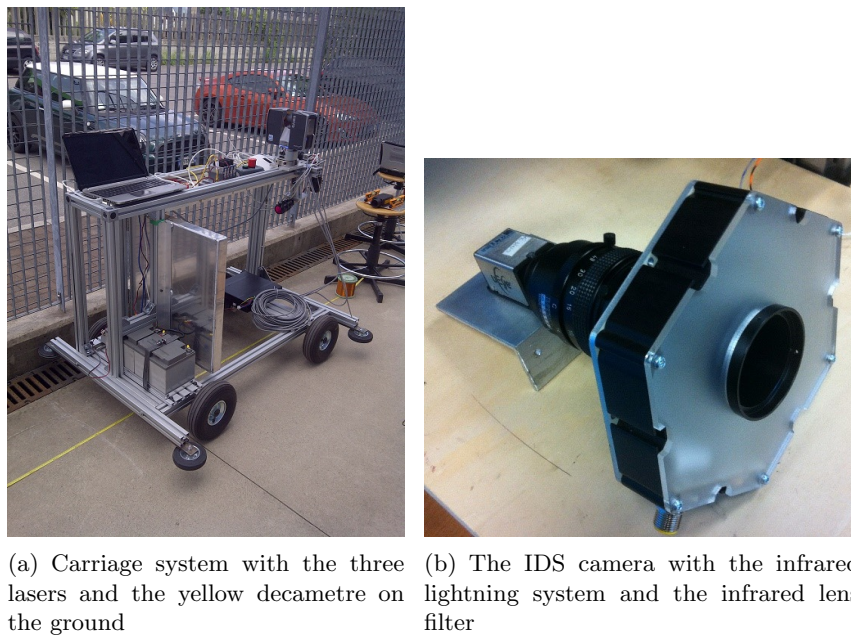


Figure 10. Setup for the {Camera 2 + Line} system

Another IDS uEye camera (identical to the previously described one) observes the metallic line. An infrared lightning system is used to illuminate the ground; the bandpass filter located on the camera reduces the influence of the environment light (Figure 10(b)).

Also in this case, images are stored by the Labview software running on the embedded PC and off-line processed. An example of the acquired images is shown in Figure 11.

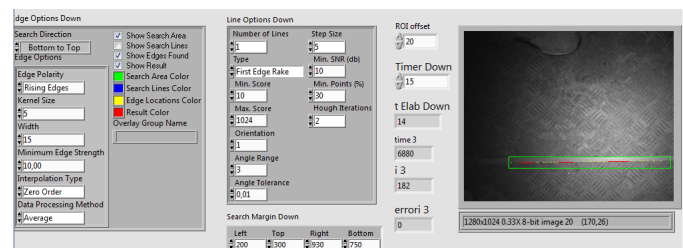


Figure 11. Labview interface for the yaw angle measurement

The angle is measured by a custom edge detection algorithm: the image is divided in columns and the grey-scale level is used to identify a point each 5 columns with an edge detection operation. Starting from the bottom of the image each column is processed with the moving average performed on a centred 15 x 5 window. All the points where the grey-scale level variation is larger than 10 are used for the edge detection. The line angle is detected by fitting these points in a least square sense. The slope is bounded between -1 and 5 degrees. Residuals are analysed to ensure that the algorithm is properly working. In addition, the region of interest for the calculation of this line is limited to ± 20 rows around the previously calculated line, since at 25 Hz the movement should not slide the line of a higher value. With this approach the image processing time is approximately 15 ms.

4.3. {Camera 3 + Line} Sideways

The same {Camera + Line} solution is used to measure the cart pitch angle, with the same hardware and image storage procedures. In this case the reference line is the handrail of the walkway, as shown in Figure 12.

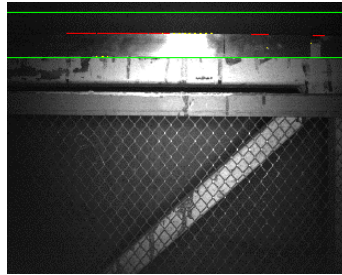


Figure 12. View of the walkway handrail, as seen by the camera

The edge used for the identification of the pitch is the one between the handrail and the background. Starting from the top of the image, the derivative of the intensity has been computed on the image averaged on a 5 x 5 window. The edge is the best line fitting the points exceeding the level of 20. The line angular coefficient is constrained between -9 and 7 degrees.

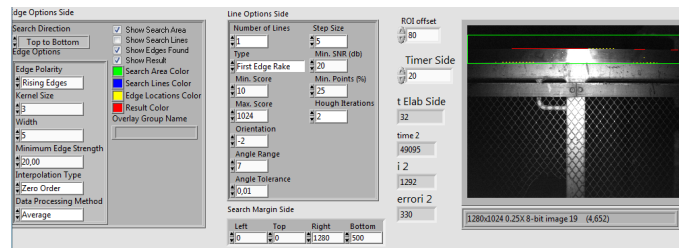


Figure 13. Labview interface for the pitch angle measurement

The analysis of the residuals helps identifying the validity of the regression procedure. The region of interest for the calculation of this line is limited to ± 80 pixels around the previously calculated line. The image processing time is approximately 30 ms. The Labview interface and parameters are shown in Figure 13.

4.4. System calibration

The system calibration is necessary for the identification of the angles and of the standoff distances between the measurement chain elements.

4.4.1. Model correction for laser beams misalignment The laser alignment is crucial for the identification of the cart motion, given that a misalignment results in a drift of the cart position and tilt. Figure 14 shows that a misalignment of the laser (θ_1 and θ_2) creates a roll angle increasing linearly with the distance x_p . The drift depends on the error Δz corresponding to a roll angle $\Delta\alpha$. The quantity $\Delta\alpha$ depends on the distance from the laser source x_p ; the mathematical model is given in equation 1.

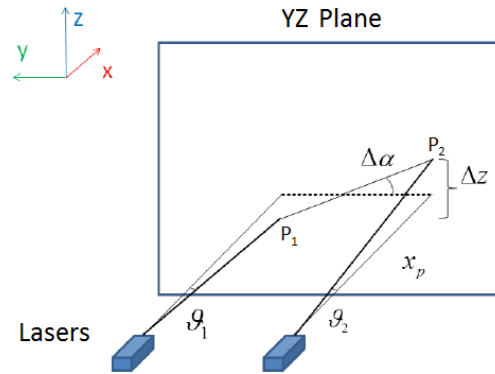


Figure 14. Misalignment of the lasers

$$\begin{aligned} \Delta\alpha &= -\arctan\left(\frac{z_{P_2} - z_{P_1}}{y_{P_2} - y_{P_1}}\right) \\ &= -\arctan\left(\frac{x_p \tan\theta_2 - x_p \tan\theta_1}{y_{P_2} - y_{P_1}}\right) \\ &\simeq -\frac{x_p (\tan\theta_2 - \tan\theta_1)}{\text{distance}(P_1 - P_2)} \quad (1) \end{aligned}$$

Since this error is systematic it can be compensated. The laser misalignment has been corrected by measuring the laser spots position at constant distances, using a linear guide as reference.

4.4.2. Intrinsic parameter of the cameras The identification of the camera parameters is crucial for the identification of the cart motion. The camera calibration consists in two steps: the first is the identification of the camera sensitivity matrix, allowing to convert the image in physical coordinates. The second is the the definition of the camera reference system, required to refer the cart motion to the global reference system.

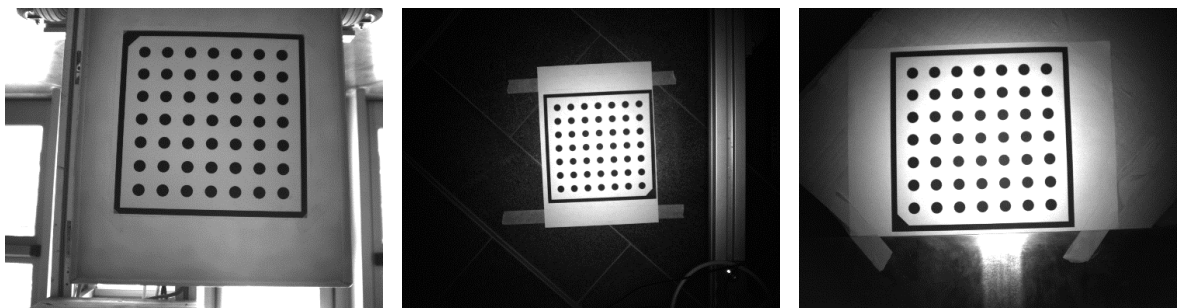


Figure 15. Laviw internal calibration of the on-board cameras

The camera sensitivity matrix has been performed with a LabVIEW-based software by acquiring a regular pattern, as shown in Figure 15.

4.4.3. *Extrinsic parameter of the cameras* The camera reference system has been identified with a static spherical scan performed by the laser scanner (as in Figure 16); the static scan obviously included both the calibration image and the camera, in order to identify the initial offset of the images.

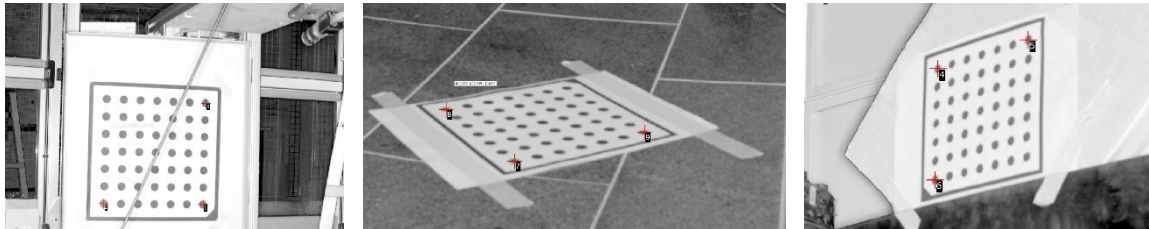


Figure 16. External calibration of the cameras respect to the laser scanner

5. Metrologic analysis - Results

5.1. Model

The system expected uncertainty has been evaluated according to the ISO - GUM indications.

- Laser Distance Meter: the resolution of 1.00 mm corresponds to a type B uncertainty of 0.29 mm.
- Camera position: the resolution of $\simeq 0.50$ mm corresponds to a type B uncertainty of 0.14 mm.
- Camera angle: the resolution of 0.01° corresponds to a type B uncertainty of 0.003° .

The measurement model is:

$$\begin{aligned} X_c &= \delta, & Roll &= \arctan\left(\frac{Z_1 - Z_3}{Y_1 - Y_3}\right) \\ Y_c &= -Y_2, & Pitch &= \alpha \\ Z_c &= -Z_2, & Yaw &= \beta \end{aligned} \quad (2)$$

where:

- $X_c, Y_c, Z_c, Roll, Pitch, Yaw$ are the components of position and orientation of the carrier in the reference frame as described in figures 5 and 7(a).
- δ the distance measured by the distance meter.
- $Y_1, Z_1, Y_2, Z_2, Y_3, Z_3$ the position of the dots in the camera frame as described in Figure 6(b).
- α, β the angles measured by the cameras respectively sideways and downwards as described in Figure 7(b).



Figure 17. Carrier at initial position during tests

5.2. Uncertainties evaluation

The theoretical uncertainties identified in the previous section have been verified with laboratory tests. Figure 10(a) shows the three lasers, the cart and the line on the ground, while Figure 17 shows the cart with a calibrator for the vision and the handrail. The cart moved forth and back following a linear path. Uncertainty has been estimated placing the cart in a known position and evaluating the position standard deviation in repeatability conditions.

Different tests has been done, in various positions along the movements. Results are summarized in table 1.

Instrument	Theoretical Uncertainty	Experimental Uncertainty
Distance Meter	1.00 mm	0.29 mm
Camera Blob	0.50 mm	0.06 mm
Camera angle	0.1°	0.04°

Table 1. Theoretical vs Experimental uncertainties

Given that the laser distance meter did not detect any variation, its uncertainty was considered equal to the theoretical one. The camera accuracy, thanks to the blob detection algorithm, was better than the theoretical one. The uncertainty of the angle is was slightly larger than the theoretical one.

Extending the result through a Monte-Carlo analysis using the previous presented model, the translation and rotation uncertainty has been evaluated and summarized in table 2.

Component	Translation Uncertainty	Rotation Uncertainty
X	0.29 mm	0.03°
Y	0.29 mm	0.04°
Z	0.06 mm	0.04°

Table 2. Translation and Orientation uncertainties

6. Conclusions

In this project, an original technique for the identification of the trajectory of a moving cart has been proposed and discussed. The solution leverages on optical systems and allowed obtaining a constant accuracy independently from the position. The theoretical uncertainty of the position is lower than 1 mm and lower than one tenth of degree for the orientation. Preliminary results were more accurate than the ones obtained with the previous system [2], but they must be verified in a real situation. The proposed method can be used in any application where it is necessary to identify the position of an object along a quasi-rectilinear path. The next step will be the test of the proposed technique in real situations for the reconstruction of a concrete bridge geometry.

References

- [1] Giberti H, Zanoni A, Mauri M and Gammino M 2014 *ASME 2014 12th Biennial Conference on Engineering Systems Design and Analysis* (American Society of Mechanical Engineers) pp V003T15A011–V003T15A011
- [2] Zanoni A, Maninetti G, Cheli F and Garozzo M 2014 *ASME 2014 12th Biennial Conference on Engineering Systems Design and Analysis* (American Society of Mechanical Engineers) pp V003T15A012–V003T15A012
- [3] Mainetti G 2011
- [4] Giancola S, Chiarion D and Sala R 2014 *Mechatronic and Embedded Systems and Applications (MESA), 2014 IEEE/ASME 10th International Conference on* (IEEE) pp 1–6
- [5] Fossati F, Sala R, Basso A, Galimberti M and Rocchi D *5th European and African Conference on Wind Engineering*